Performance evaluation of a 640-Gbps integrated dense wavelength division multiplexing-mode division multiplexing-based free-space optics transmission system

KARAMJEET SINGH[1], MEHTAB SINGH[2,*], AMIT GROVER[1]
[1]*Department of Electronics and Communication Engineering, Shaheed Bhagat Singh State University, Punjab, India*
[2]*Department of Electronics and Communication Engineering, University Institute of Engineering, Chandigarh University, Mohali, Punjab, India*

This study presents the modeling of a terrestrial free-space optics (FSO) transmission system that integrates mode division multiplexing (MDM) with dense wavelength division multiplexing (DWDM). A total of 32 laser channels, operating within the frequency range of 193.1 THz to 196.2 THz, are utilized. The channels are spaced apart by 100 GHz. Each wavelength channel employs two spatial Hermite-Gaussian (HG) modes, specifically $HG_{0,1}$ and $HG_{1,1}$. These modes are responsible for transmitting 10-Gbps of non-return-to-zero data. The transmission takes place over a free-space channel, even in challenging weather conditions. The system's net transmission speed is 640 Gbps. The FSO system is assessed for its performance under several weather conditions, including clear, rain, haze, and fog using simulative analysis. The metrics used for evaluation are the signal-to-noise ratio, received power, and eye diagrams. The findings exhibit consistent transmission at a speed of 640 Gbps over a range of 800 meters to 6 kilometers, with dependable performance metrics.

(Received January 26, 2024; accepted June 5, 2024)

Keywords: Mode division multiplexing, Hermite-Gaussian modes, Dense wavelength division multiplexing, Free-space optics, Weather attenuation

1. Introduction

Free Space Optics (FSO) is based on the notion of sending data through unobstructed space utilizing beams of light. This is accomplished by utilizing lasers or light-emitting diodes (LEDs) to produce modulated optical signals, which are subsequently directed into the environment. The transmission relies on the line-of-sight communication concept, wherein the signal propagates directly from the transmitter to the receiver, facilitating efficient communication across limited to moderate distances [1, 2]. FSO systems possess numerous noteworthy benefits. These systems offer fast and significant data transfer, often achieving speeds of up to hundred gigabit per second, which is particularly useful for applications that demand quick and large-scale data transfer. Furthermore, FSO functions inside the optical spectrum that does not require a license, which enhances cost efficiency and simplifies the process of implementation. The technology is impervious to radio frequency (RF) interference, guaranteeing a dependable and protected communication connection. FSO systems are renowned for their rapid deployment, making them highly suitable for situations such as temporary communication links or emergency installations [3-5]. In addition, the low-latency characteristic of FSO enables the use of real-time applications. FSO is utilized in diverse situations because of its distinctive characteristics. It is frequently used in urban communication networks, providing a wireless option for connecting the final stretch. FSO systems are employed in corporate networks to establish fast data connections between different buildings or campuses [6]. FSO enables secure and uninterrupted communication in military and defense contexts. Moreover, FSO is utilized in scenarios involving the restoration of operations after a disaster and in the establishment of temporary communication systems, thereby demonstrating its adaptability in many settings [7-10].

Although FSO possesses notable advantages, it is not exempt from constraints. An important obstacle is the system's susceptibility to atmospheric circumstances, namely unfavorable weather conditions like intense rainfall, fog, or snow, which can weaken the optical signal and diminish its effectiveness [11-13]. The presence of barriers such as buildings or topography might impede the optical path, hence imposing constraints on the line-of-sight requirement. Furthermore, FSO systems may encounter signal deterioration while transmitting over extended distances [14]. Addressing these problems is essential for fully harnessing the potential of FSO technology in diverse practical applications.

A lot of research is being carried out to increase the information transmission rate in FSO systems. Dense Wavelength Division Multiplexing (DWDM) is a widely used method in optical fiber communication that allows for the simultaneous transmission of numerous data streams over a single optical cable. DWDM accomplishes this by using distinct wavelengths of light to transport separate data channels. Every individual wavelength has

the capability to accommodate a substantial amount of data, leading to a higher overall capacity of the system. By incorporating DWDM technology into FSO systems, the spectral efficiency of these systems is improved [15]. This offers a solution to meet the increasing need for data-intensive applications. The authors in [16] have discussed the implementation of DWDM transmission in FSO environment by incorporating hybrid on-off keying/ digital-pulse-position modulation schemes. The results demonstrated transmission of 8 DWDM channels across adverse environment to achieve 20 Gbps net transmission rate. The investigation of hybrid single-mode-fibre/FSO transmission by incorporating DWDM transmission over 5 km link range is discussed by authors in [17]. Improved performance analysis of DWDM based passive optical network using modified on-off-keying modulation across various environmental conditions in hybrid fibre/FSO transmission is reported in [18]. The implementation of DWDM transmission with multi-input multi-output techniques and diverse coding techniques to enhance the FSO transmission performance under adverse weather conditions is discussed in [19]. DWDM transmission in hybrid RF/FSO link by incorporating spatial pulse position modulation is reported in [20]. Performance evaluation of hybrid RF/FSO link over Malaga distribution model is discussed in [21]. Mode Division Multiplexing (MDM) is a nascent technology that utilizes several modes of a multimode optical cable to send distinct data streams autonomously. MDM increases the capacity of optical communication systems by employing different modes that travel through the fiber. MDM integration with FSO systems enables the concurrent transmission of several data streams across a single optical route, resulting in enhanced overall system throughput [22-25]. The use of orbital-angular-momentum spatial multiplexing, which is a form of MDM, to improve the performance of FSO transmission under turbulence effect is reported in [26].

The combination of DWDM and MDM in FSO systems offers an effective solution to meet the increasing need for faster data rates and enhanced communication dependability. This integrated methodology combines the ability to transmit a large amount of data per unit of bandwidth (spectral efficiency) of DWDM with the advantage of having multiple spatial channels (spatial diversity) afforded by MDM. As a result, there is a significant enhancement in both the total capacity and resilience of FSO systems. This study explores performance evaluation of a FSO system using integrated DWDM-MDM technologies under the effect of different weather conditions. Section 2 discusses the system setup, followed by results and discussion in Section 3 and the final conclusion in Section 4.

2. System design

The system schematic of the proposed DWDM-MDM-FSO transmission link, designed using Optisystem software version 21.0 is shown in Fig. 1.

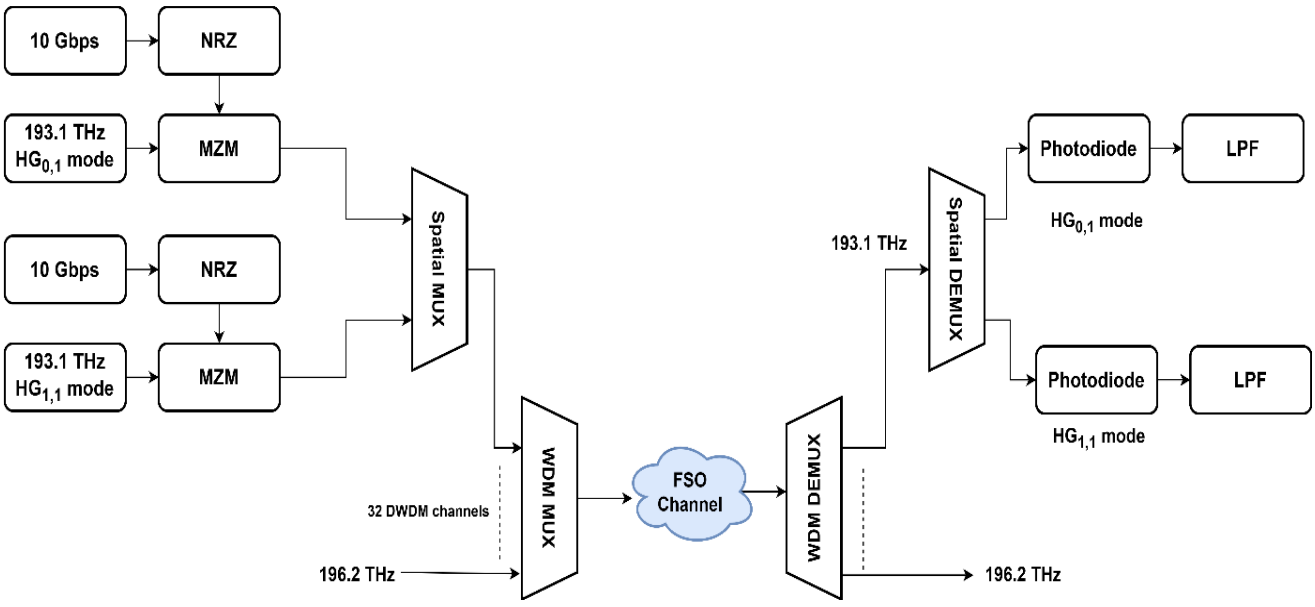

Fig. 1. Proposed DWDM-MDM system schematic

The study incorporates 32 DWDM channels, spanning from 193.1 THz to 196.2 THz, with a channel separation of 100 GHz. Each wavelength channel employs two MDM-Hermite-Gaussian (HG) modes, specifically $HG_{0,1}$ and $HG_{1,1}$. Every HG mode carries 10 Gbps of non-return-to-zero (NRZ) data. The total transmission speed of the system is calculated as 32λ×2 spatial HG modes× 10 Gbps, resulting in a speed of 640 Gbps.

In the transmitter part, the input data with a speed of 10 Gbps is encoded using NRZ technique and then modulated onto a specific HG mode with a frequency of 193.1 THz. Different HG modes are generated using

mode-generator component in Optisystem simulation software. The HG mode can be mathematically represented as [27]:

$$\psi_{m,n}(r,\varphi) = H_m\left(\frac{\sqrt{2}x}{w_{0x}}\right)\exp\left(-\frac{x^2}{w_{0x}^2}\right)\exp\left(j\frac{\pi x^2}{\lambda R_{0x}}\right) H_n\left(\frac{\sqrt{2}y}{w_{0y}}\right)\exp\left(-\frac{y^2}{w_{0y}^2}\right)\exp\left(j\frac{\pi y^2}{\lambda R_{0y}}\right) \quad (1)$$

where, H_m and H_n represent Hermite polynomials, m and n represent mode dependencies on x- and y- axis respectively, R represents the curvature radius, and w_0 represents the size of the beam at the waist. 2-optically modulated HG beams i.e., $HG_{0,1}$ and $HG_{1,1}$ are multiplexed using a spatial multiplexer. Fig. 2 elucidates the spatial profile of HG beams.

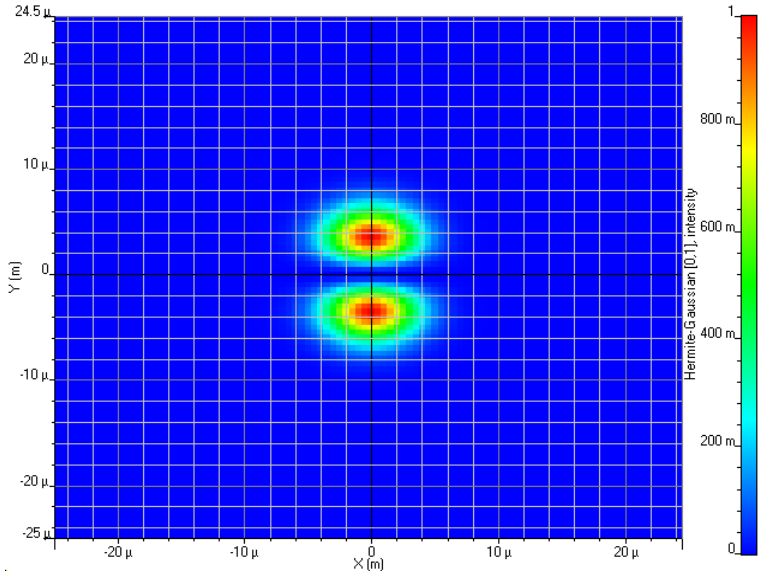

(a)

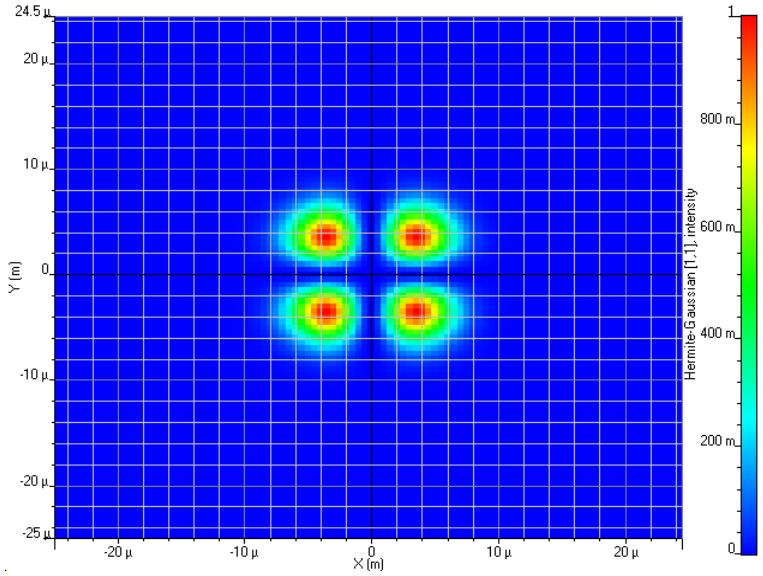

(b)

Fig. 2. (a) $HG_{0,1}$ (b) $HG_{1,1}$ spatial beam intensity profiles (color online)

The Spatial WDM multiplexer (MUX) combines the spatial modes of all the 32-wavelength channels spanning from 193.1 THz to 196.2 THz. The 640-Gbps information transmission is transmitted through the channel of free space. The laser beam carrying information is subject to attenuation caused by various weather conditions. The optical power that is received can be represented by the following equation:

$$S_R = S_T\left(\frac{d_r^2}{(d_t + \theta Z)^2}\right)10^{-\sigma Z/10} \quad (2)$$

where,

S_R: Received optical power
S_T: Transmitted optical power
d_r: Receiver antenna diameter
d_t: Transmitter antenna diameter
σ: Attenuation coefficient
Z: FSO range

Table 1 presents the simulation parameters that were taken into account in this study.

Table 1. Simulation parameters [28 - 30]

Parameters	Value
Laser frequency band	193.1 – 196.2 THz
Channel spacing	100 GHz
Power of each laser	10 dBm
Linewidth	10 MHz
Extinction ratio	10 dB
Bitrate per channel	10 Gbps
d_r	5 cm
d_t	20 cm
θ	0.25 $mrad$
Turbulence model	Gamma-Gamma
Scintillation [20]	$5 \times 10^{-17}\ m^{-2/3}$
Thermal power density of photodiode	100e-024 W/Hz
Responsivity	0.7 A/W
WDM MUX Bandwidth	100 GHz
Attenuation coefficient	0.14 dB/km (Clear)

At the receiver part, the 640-Gbps optical signal is separated into 32 individual wavelengths using a Spatial WDM demultiplexer. In addition, the MDM demultiplexer is employed to spatially demultiplex each DWDM channel. The 10-Gbps optical channel is initially transformed into an electrical signal using a PIN photodiode. Subsequently, a low pass filter (LPF) is employed to eliminate the noise frequency. Table 2 presents the attenuation coefficient for various weather conditions examined in this study. The optical spectra of the sent signal and the received signal are illustrated in Fig. 3 (a) and (b) accordingly.

Table 2. Weather attenuation coefficient [29, 30]

	Attenuation in dB/km		
	Light	Medium	Heavy
Haze	1.537	4.285	10.115
Rain	6.27	9.64	19.28
Fog	9	16	22

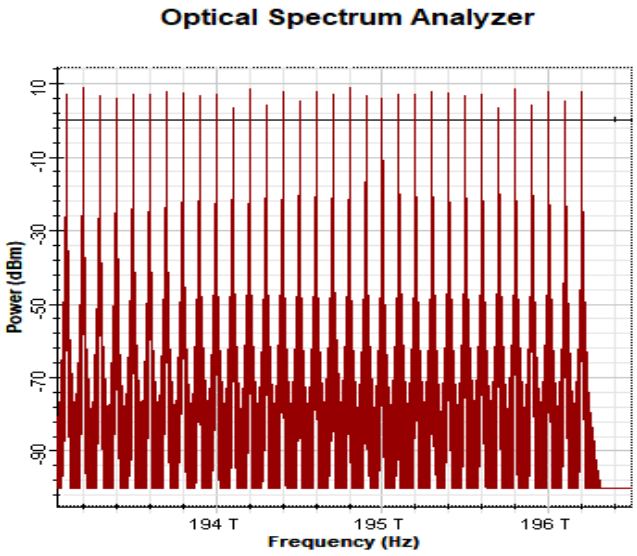

(a)

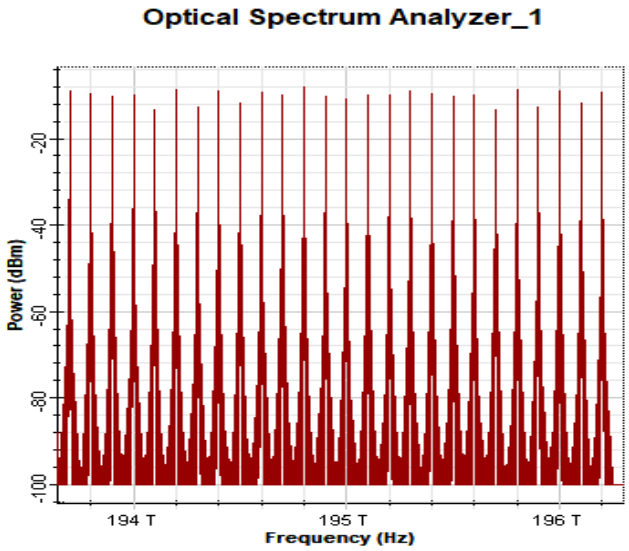

(b)

Fig. 3. Optical spectra of (a) Transmitted (b) Received signal

3. Results and discussions

The performance of the proposed DWDM-MDM-FSO transmission system is evaluated under different weather conditions. Since all the channels report similar performance, we show shown the plots for channel 1 (193.1 THz-$HG_{0,1}$ mode only). Fig. 4 (a) and (b) illustrate the signal-to-noise ratio (SNR) and received power plots versus increasing FSO range for clear sky weather at different beam divergence angle. The reported SNR is 38.55, 26.75, and 19.43 dB for 0.25 mrad divergence angle; 27.31, 15.13, and 7.67 dB for 0.50 mrad divergence angle; and 20.55, 8.23, and 0.72 dB for 0.75 mrad divergence angle at 2, 4, and 6 km FSO range respectively.

The reported received power is -61.44, -73.24, and -80.56 dBm for 0.25 mrad divergence angle; -72.68, -84.86, and -92.31 dBm for 0.50 mrad divergence angle; and -79.44, -91.75, and -99.19 dBm for 0.75 mrad divergence angle at 2, 4, and 6 km FSO range respectively. From the results, it is observed that as the beam divergence increases, the signal degrades. As the beam carrying information diverges, lesser amount of optical beam is captured by the lens at the receiver terminal. As a result, the signal power reduces and the quality of the signal degrades. Further, on increasing the FSO range, the signal quality deteriorates. The maximum FSO reach achieved can be observed as 6 km for 0.25 mrad divergence, 3 km for 0.50 mrad divergence, and 2 km for 0.75 mrad divergence angle. Fig. 5 illustrates the eye diagram of the received signal at 6 km under clear weather.

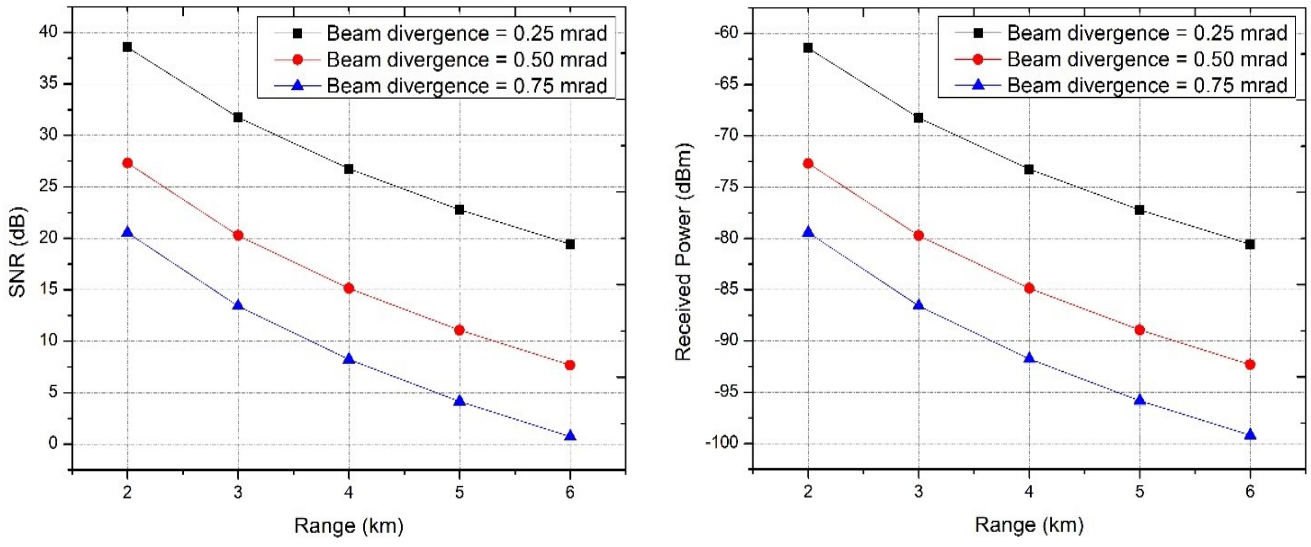

(a) (b)

Fig. 4. (a) SNR (b) Received power v/s FSO Range under clear weather (color online)

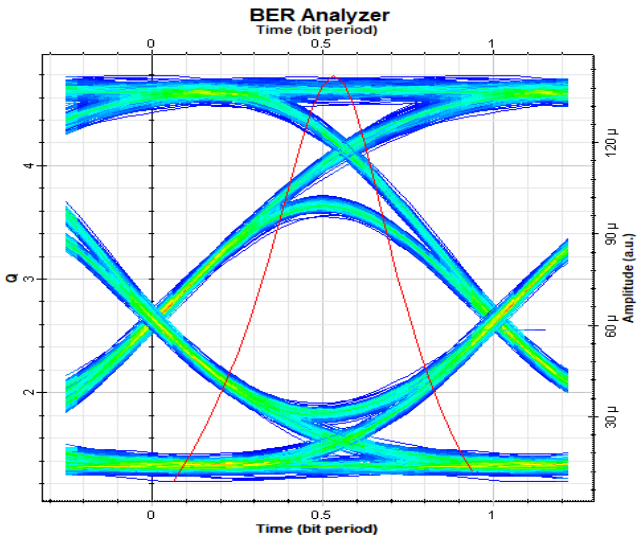

Fig. 5. Eye diagram of the received signal at 6 km range under clear weather (color online)

Fig. 6 illustrates the performance of the proposed transmission under varying rain weather conditions. The reported SNR is 39.86, 28.26, and 18.19 dB at 900, 1350, and 1800 m respectively for light rain conditions; 41.14, 30.36, and 20.70 dB at 700, 1000, and 1300 m respectively for medium rain conditions; and 38.46, 28.80, and 19.73 dB at 520, 680, and 840 m respectively for heavy rain conditions. The reported received power is -60.13, -71.73, and -81.80 dBm at 900, 1350, and 1800 m respectively for light rain conditions; -58.85, -69.63, and -79.29 dBm at 700, 1000, and 1300 m respectively for medium rain conditions; and -61.53, -71.19, and -80.26 dBm at 520, 680, and 840 m respectively for heavy rain conditions. Fig. 7 illustrates the eye diagrams of the received signal under different rain conditions.

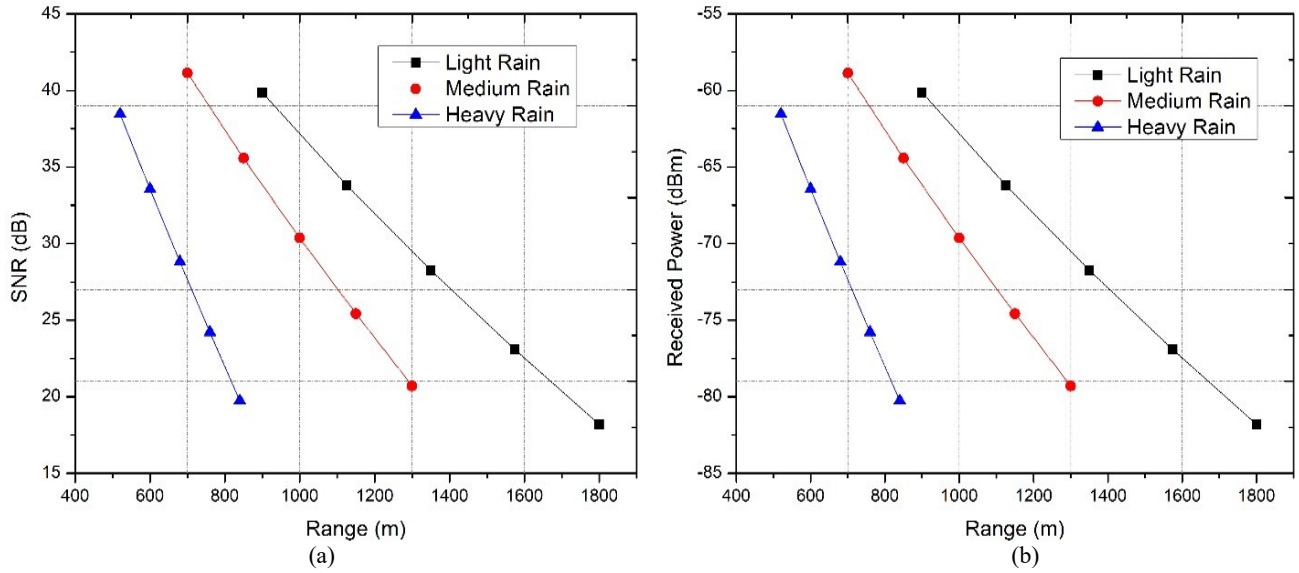

Fig. 6. (a) SNR (b) Received power v/s range under rain conditions (color online)

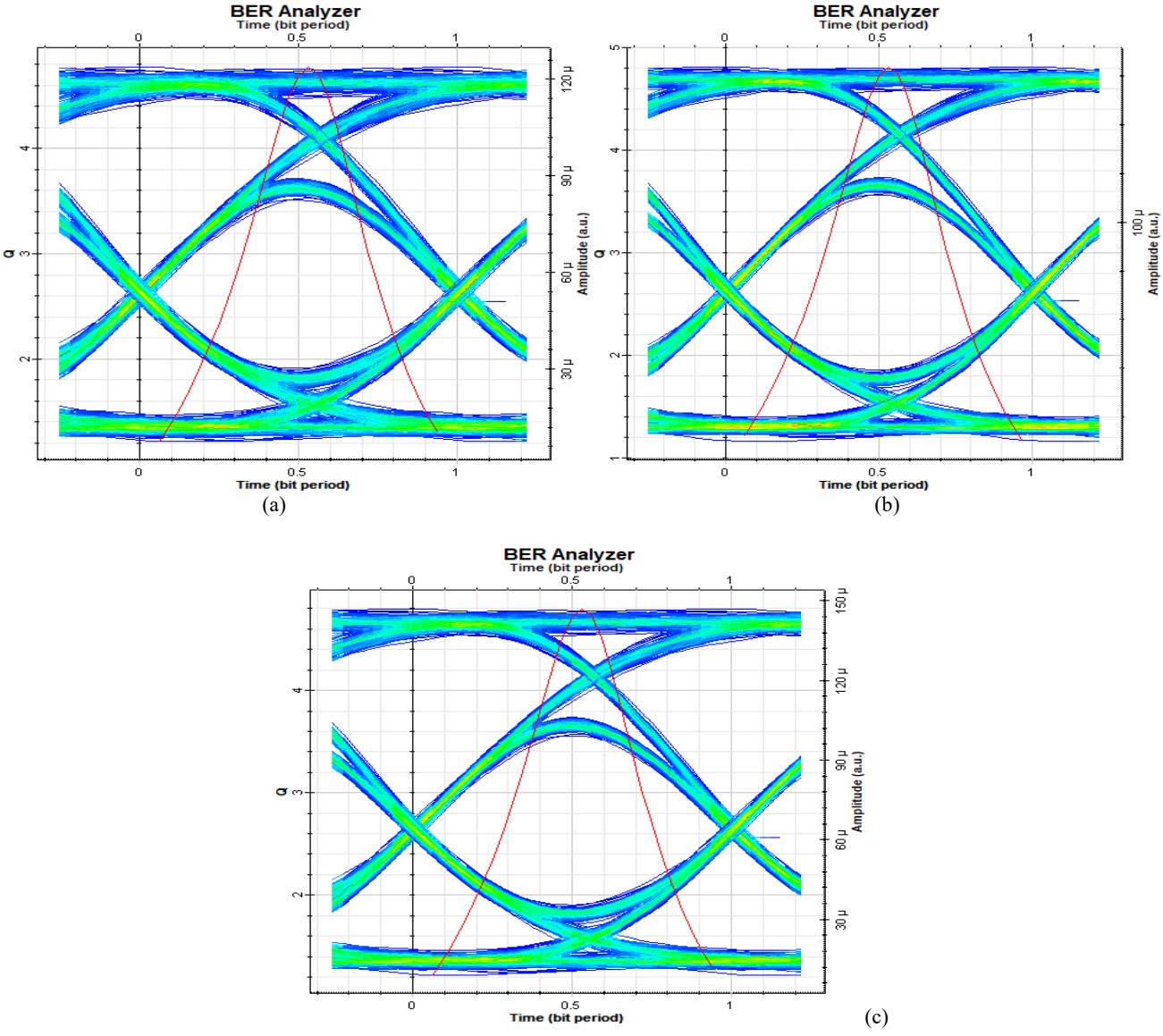

Fig. 7. Eye diagram at (a) 1800 m (Light Rain) (b) 1300 m (Medium Rain) (c) 840 m (Heavy Rain) (color online)

Fig. 8 illustrates the performance of the proposed transmission under varying haze weather conditions. The reported SNR is 37.67, 26.93, and 18.55 dB at 1600, 2600, and 3600 m respectively for light haze conditions; 37.73, 27.98, and 19.54 dB at 1150, 1650, and 2150 m respectively for medium haze conditions; and 37.76, 27.01, and 17.25 dB at 770, 1070, and 1370 m respectively for heavy haze conditions. The reported received power is -62.32, -73.06, and -81.44 dBm at 1600, 2600, and 3600 m respectively for light haze conditions; -62.26, -72.01, and -80.45 dBm at 1150, 1650, and 2150 m respectively for medium haze conditions; and –62.23, -72.98, and -82.74 dBm at 770, 1070, and 1370 m respectively for heavy haze conditions. Fig. 9 illustrates the eye diagrams of the received signal under different haze conditions.

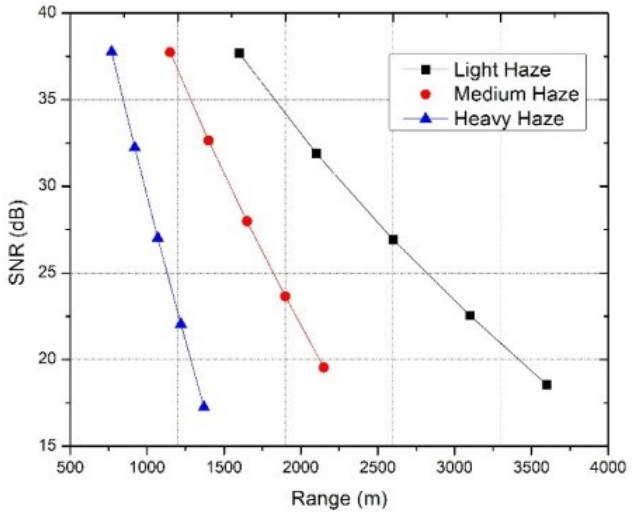

(a)

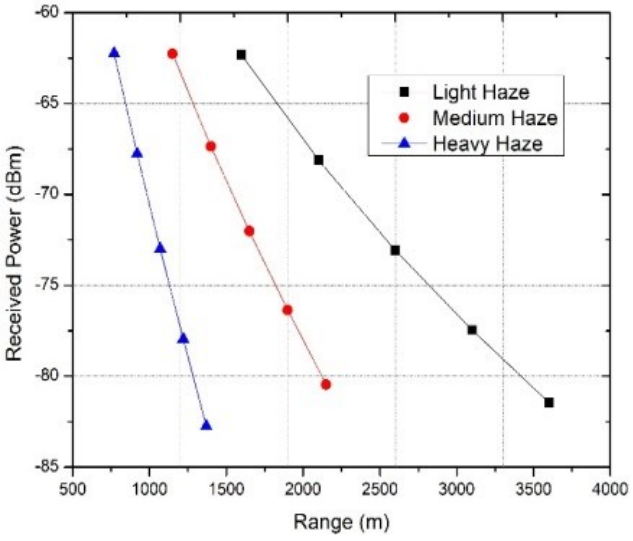

(b)

Fig. 8. (a) SNR (b) Received power v/s range under haze conditions (color online)

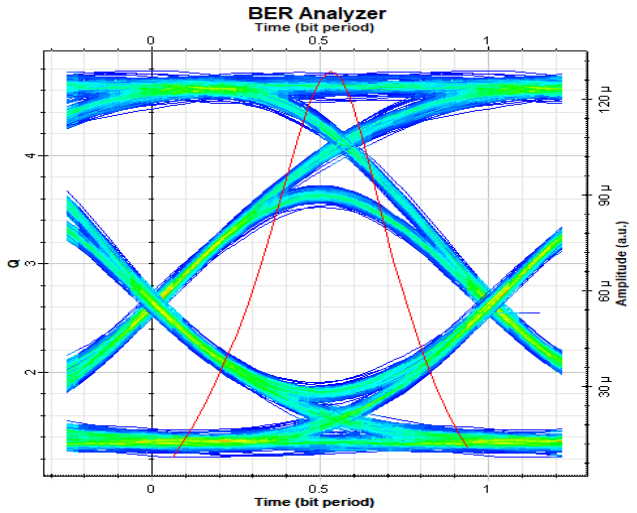

(a)

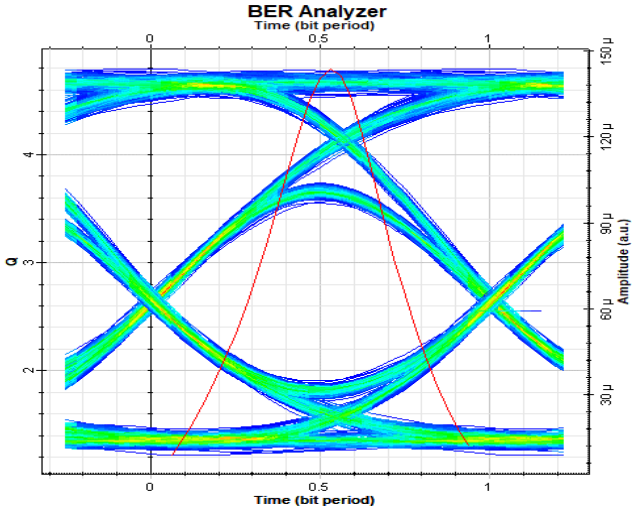

(b)

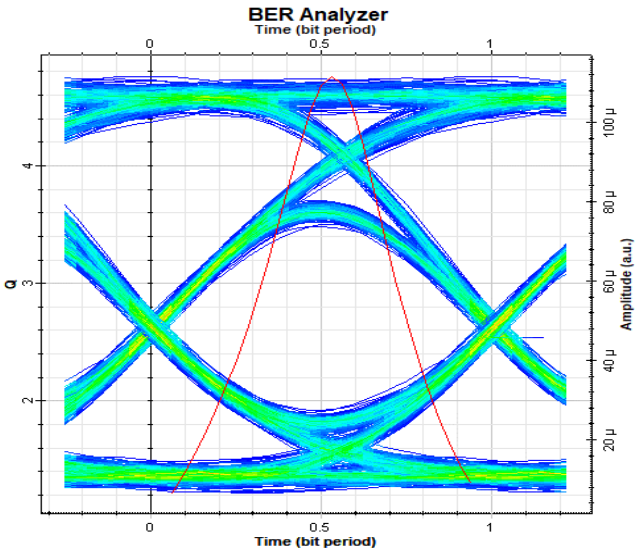

(c)

Fig. 9. Eye diagram at (a) 3600 m (Light Haze) (b) 2150 m (Medium Haze) (c) 1370 m (Heavy Haze) (color online)

Fig. 10 illustrates the performance of the proposed transmission under varying fog weather conditions. The reported SNR is 36.66, 26.89, and 18.00 dB at 850, 1150, and 1450 m respectively for light fog conditions; 36.15, 27.20, and 18.80 dB at 625, 800, and 975 m respectively for medium fog conditions; and 37.00, 27.03, and 17.60 dB at 500, 650, 800 m respectively for heavy fog conditions. The reported received power is -63.33, -73.10, and -81.98 dBm at 850, 1150, and 1450 m respectively for light fog conditions; -63.84, -72.79, and -81.19 dBm at 625, 800, and 975 m respectively for medium fog conditions; and -62.99, -72.96, and -82.38 dBm at 500, 650, and 800 m respectively for heavy fog conditions. Fig. 11 illustrates the eye diagrams of the received signal under different fog conditions.

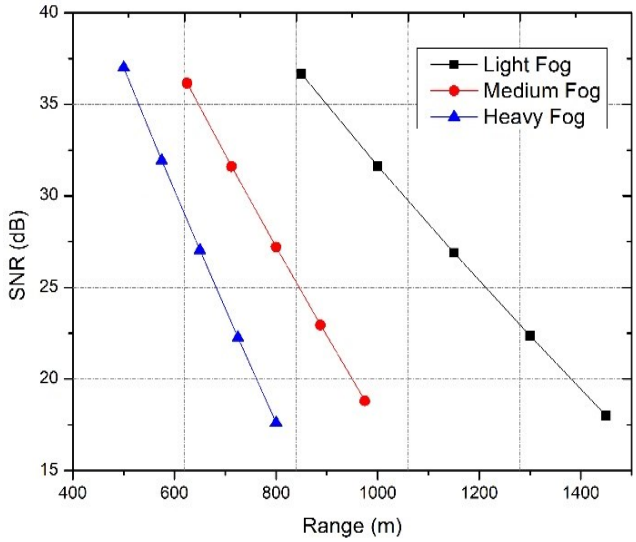

(a)

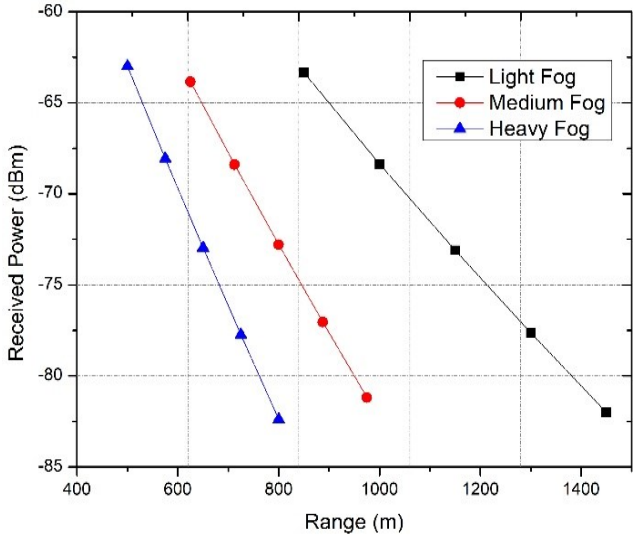

(b)

Fig. 10. (a) SNR (b) Received power v/s range under fog conditions (color online)

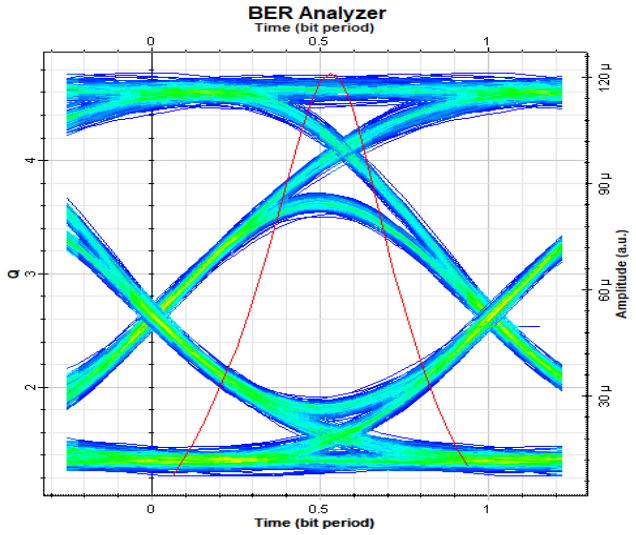

(a)

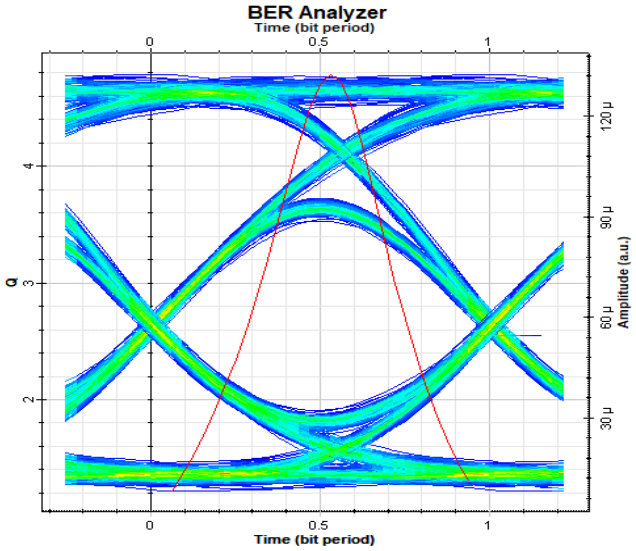

(b)

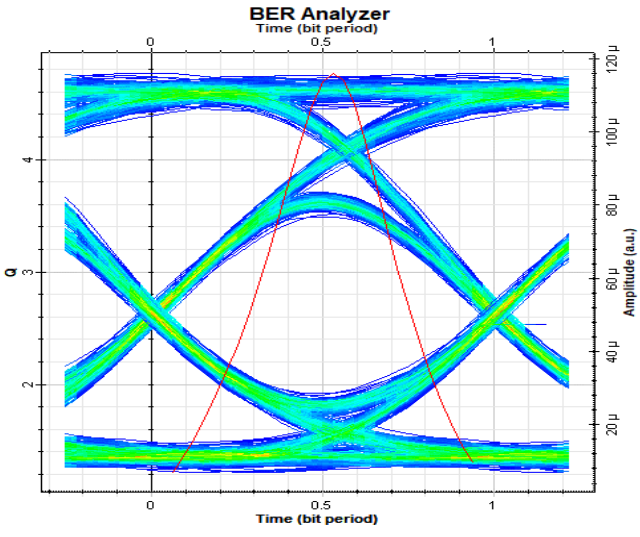

(c)

Fig. 11. Eye diagram at (a) 1450 m (Light Fog) (b) 975 m (Medium Fog) (c) 800 m (Heavy Fog) (color online)

From the results across different weather scenarios, it can be seen that as the attenuation increases due to adverse weather condition, the signal quality in terms of Q Factor, SNR, and Received power degrades due to lesser power at the receiver terminal which deteriorates the link quality. Table 3 presents the highest attained FSO range under various weather circumstances, while maintaining a satisfactory SNR for the received signals.

Table 3. Maximum achieved FSO range

Weather	Maximum achieved range
Clear	6 km
Light Fog	1450 m
Light Haze	3600 m
Light Rain	1800 m
Medium Fog	975 m
Medium Haze	2150 m
Medium Rain	1300 m
Heavy Fog	800 m
Heavy Haze	1370 m
Heavy Rain	840 m

4. Conclusion

We have presented a new and advanced high-speed integrated transmission system that combines MDM (mode division multiplexing), DWDM (dense wavelength division multiplexing), and FSO (free-space optical) technologies. The transmission system employs two spatial HG modes across 32 distinct wavelength channels to transport 10 Gbps data for 64 users, resulting in a total transmission rate of 640 Gbps. The system under consideration is assessed under various environmental circumstances, resulting in a range of 6 km in clear conditions. In light fog, the range achieved is 1450 m, while in light haze and light rain, the ranges are 3600 m and 1800 m respectively. In medium fog, the range achieved is 975 m, while in medium haze and medium rain, the ranges are 2150 m and 1300 m respectively. In heavy fog, the range achieved is 800 m, while in heavy haze and heavy rain, the ranges are 1370 m and 840 m respectively. The proposed approach can be employed to fulfill the demand for high data transmission rates in 5G/6G networks.

References

[1] S. A. Al-Gailani, M. F. M. Salleh, A. A. Salem, R. Q. Shaddad, U. U. Sheikh, N. A. Algeelani, T. A. Almohamad, IEEE Access **9**, 7353 (2021).

[2] M. Goncalves Teixeira, J. R. Molina, V. N. G. J. Soares, Electronics **10**, 1607 (2021).

[3] Sarmistha Satrusalya, Laxmi Goswami, Materials Today: Proceedings, **81**, Part 2, 231 (2023).

[4] Aditi Malik, Preeti Singh, International Journal of Optics **2015**, Article ID 945483 (2015).

[5] In Keun Son, Shiwen Mao, Digital Communications and Networks **3**(2), 67 (2017).

[6] P. Kulshreshtha, A. K. Garg, **2020** 11th International Conference on Computing, Communication and Networking Technologies (ICCCNT), Kharagpur, India, 1 - 4 (2020).

[7] G. Zhang, J. Wu, Y. Li, X. Wang, X. Yu, S. Gao, L. Ma, Photonics **10**, 756 (2023).

[8] Arun K. Majumdar, Advanced Free Space Optics (FSO): A Systems Approach, Springer, New York, 2015.

[9] M. R. Hayal, E. E. Elsayed, D. Kakati, M. Singh, A. Elfikky, A. I. Boghdady, A. Gupta, S. Mehta, S. A. H. Mohsan, I. Nurhidayat, Opt. Quant. Electron. **55**, 625 (2023).

[10] E. E. Elsayed, Opt. Quant. Electron. **56**, 837 (2024).

[11] M. A. Khalighi, M. Uysal, IEEE Communications Surveys & Tutorials **16**(4), 2231 (2014).

[12] Arun K. Majumdar, Jennifer C. Ricklin, Free-Space Laser Communications: Principles and Advances, Springer, New York, 2008.

[13] Hemani Kaushal, Georges Kaddoum, IEEE Communications Surveys & Tutorials **19**(1), 57 (2017).

[14] A. J. Seeds, H. Shams, M. J. Fice, C. C. Renaud, Journal of Lightwave Technology **33**(3), 579 (2015).

[15] D. E. Mohsen, E. M. Abbas, M. M. Abdulwahid, **2022** International Congress on Human-Computer Interaction, Optimization and Robotic Applications (HORA), Ankara, Turkey 1 (2022).

[16] E. E. Elsayed, D. Kakati, M. Singh, A. Grover, G. Anand, Opt. Quant. Electron. **54**, 768 (2022).

[17] E. E. Elsayed, A. G. Alharbi, M. Singh, A. Grover, Opt. Quant. Electron. **54**, 358 (2022).

[18] E. E. Elsayed, B. B. Yousif, Opt. Quant. Electron. **52**, 385 (2020).

[19] E. E. Elsayed, M. R. Hayal, I. Nurhidayat, M. A. Shah, A. Elfikky, A. I. Boghdady, D. A. Juraev, M. A. Morsy, IET Optoelectron. **18**(1-2), 11 (2024).

[20] Ebrahim E. Elsayed, Optics Communications **562**, 130558 (2024).

[21] Narendra Vishwakarma, R. Swaminathan, Optics Communications **487**, 126796 (2021).

[22] S. Chaudhary, L. Wuttisittikulkij, J. Nebhen, X. Tang, M. Saadi, S. Al Otaibi, A. Althobaiti, A. Sharma, S. Choudhary, Front. Phys. **9**, 756232 (2021).

[23] S. Srivastava, K. K. Upadhyay, N. Singh, Indian J. Phys. **94**, 1803 (2020).

[24] M. Singh, S. Chebaane, S. Ben Khalifa, A. Grover, S. Dewra, M. Angurala, Front. Phys. **9**, 746779 (2021).

[25] A. Grover, A. Sheetal, "Performance Investigation of 4 × 20 Gbit/S-40 GHz MDM-OFDM-FSO System Under Weather Conditions" in: S. Smys, R. Palanisamy, Á. Rocha, G. N. Beligiannis, (eds) Computer Networks and Inventive Communication Technologies. Lecture Notes on Data Engineering and Communications Technologies **58**, Springer, Singapore, 2021.

[26] B. B. Yousif, E. E. Elsayed, IEEE Access **7**, 84401 (2019).

[27] A. Ghatak, K. Thyagarajan, "Introduction to Fiber Optics", Cambridge University Press, New York, NY, 1998.
[28] S. Chaudhary, B. Lin, X. Tang, X. Wei, Z. Zhou, C. Lin, M. Zhang, H. Zhang, Opt. Quant. Electron. **50**, 321 (2018).
[29] S. Chaudhary, L. Wuttisittikulkij, J. Nebhen, X. Tang, M. Saadi, S. Al Otaibi, A. Althobaiti, A. Sharma, S. Choudhary, Front. Phys. **9**, 756232 (2021).
[30] Yogesh Kumar Gupta, Aditya Goel, Heliyon **9**(2), e13325 (2023).

*Corresponding author: mehtab91singh@gmail.com